Start-to-End Beam Dynamics Optimization of X-Ray FEL Light Source Accelerators

Ji Qiang

North American Particle Accelerator Conference, Chicago,
Oct. 9 -14, 2016

Outline

- Introduction
- Parallel multi-objective global optimization method
- Start-to-end FEL accelerator beam dynamics optimization
- Application to an LCLS-II design study
- Conclusions

X-Ray FEL Based Light Sources Provide Great Opportunity for Scientific Discovery

Natural and Artificial Photosynthesis

Fundamental Charge Dynamics

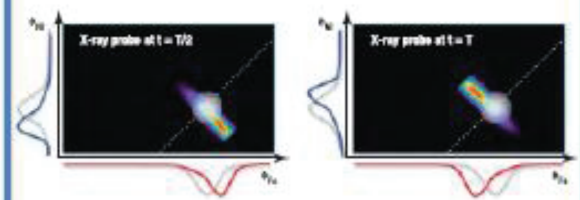

Advanced Combustion Science

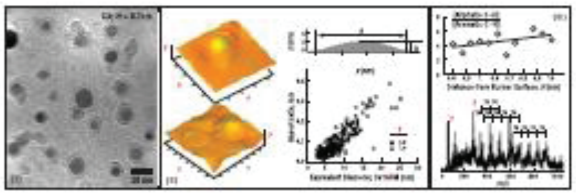

Catalysis

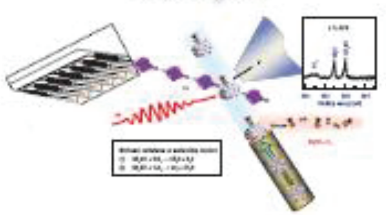

Nanoscale Materials Nucleation

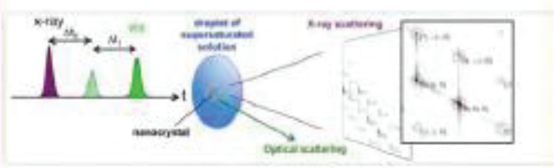

Dynamic Nanoscale Heterogeneity

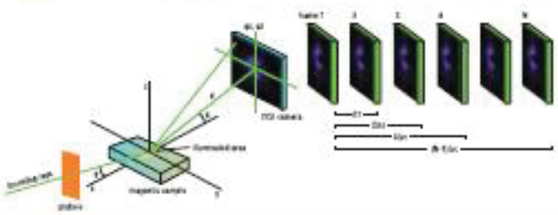

Quantum Materials

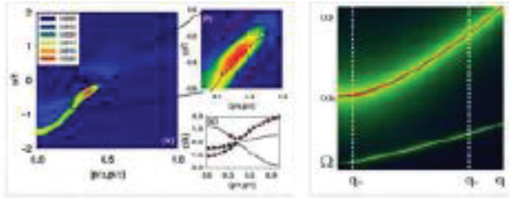

Nanoscale Spin and Magnetization

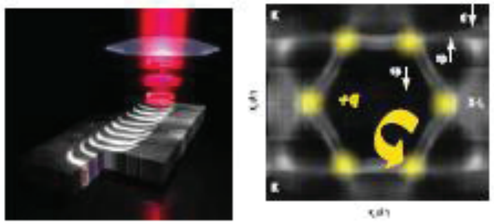

Bioimaging: Structure-to-Function

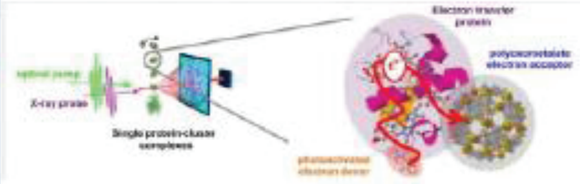

Courtesy of R. Scholenlein

Some X-Ray FEL User Facilities in the World

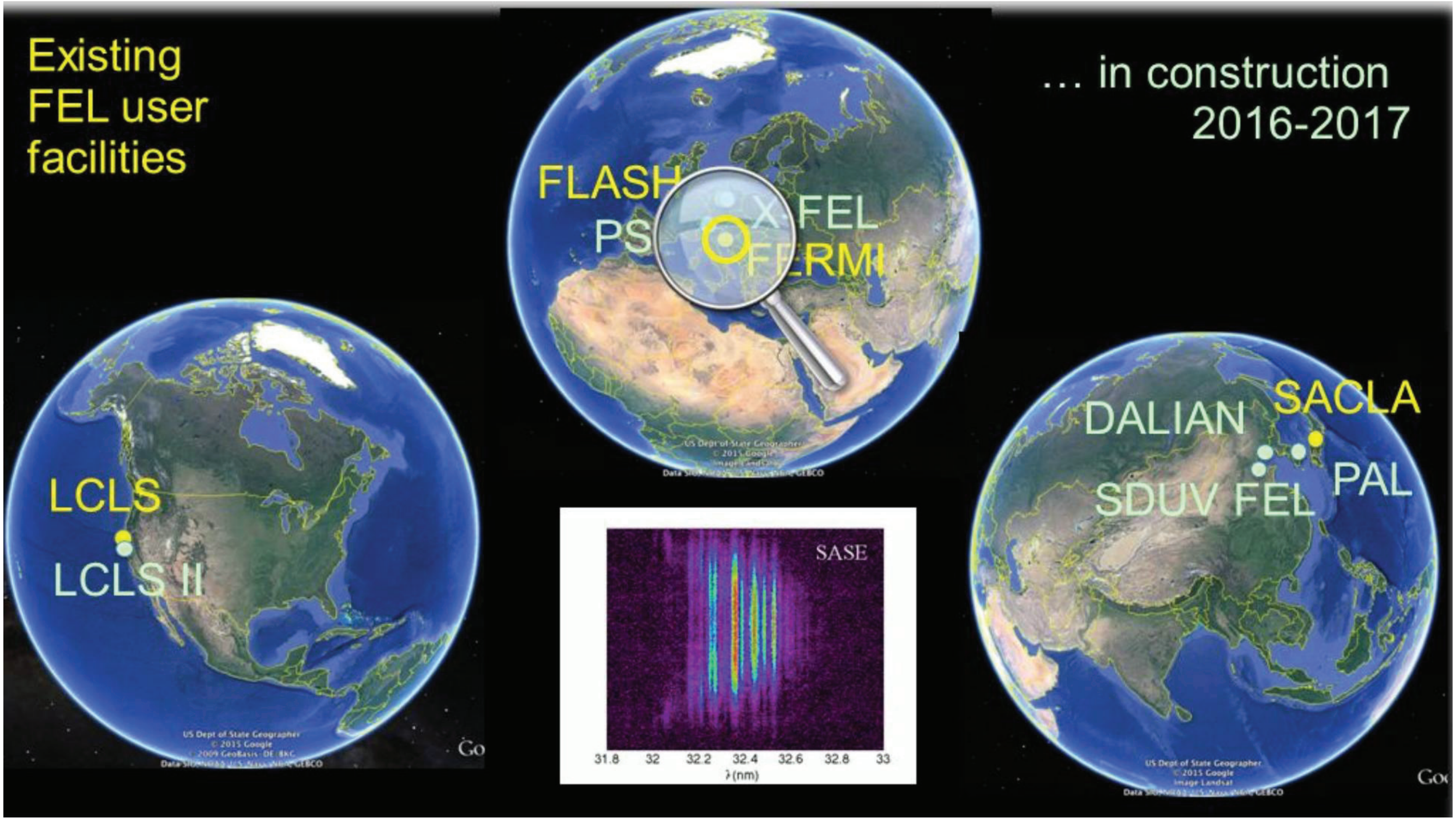

Courtesy of L. Gannessi

The FEL Cost and Performance Critically Depend on Electron Beam Quality

- **Electron beam emittance ε**

$$\frac{\varepsilon_n}{\gamma} \approx \frac{\lambda_{x-ray}}{4\pi} \qquad \lambda_{x-ray} = \frac{\lambda_{undulator}}{2\gamma^2}\left(1+\frac{K^2}{2}\right)$$

- **Peak current I_{peak}**

$$P_{sat} \approx 1.6\rho\left(\frac{L_{G,1D}}{L_G}\right)^2 P_{b,pk} \qquad P_{b,pk} = I_{pk}\,\gamma\, mc^2/e$$

$$\rho = \left(\frac{1}{16}\frac{I_{pk}}{I_A}\frac{K^2[JJ]^2\lambda_u^2}{4\pi^2\gamma^3\sigma_x^2}\right)^{1/3}$$

- **Gain length**

$$L_{G0} = \frac{\lambda_u}{4\pi\sqrt{3}\rho}$$

- **Energy spread σ_E**

$$\Delta\omega = \frac{2\sigma_\gamma/\gamma}{\lambda_r}c$$

Ideal electron beam:
- high peak current
- small energy spread
- small emittance

Global Start-to-End Beam Dynamics Optimization Is Needed to Achieve the "Best" Electron Beam Quality

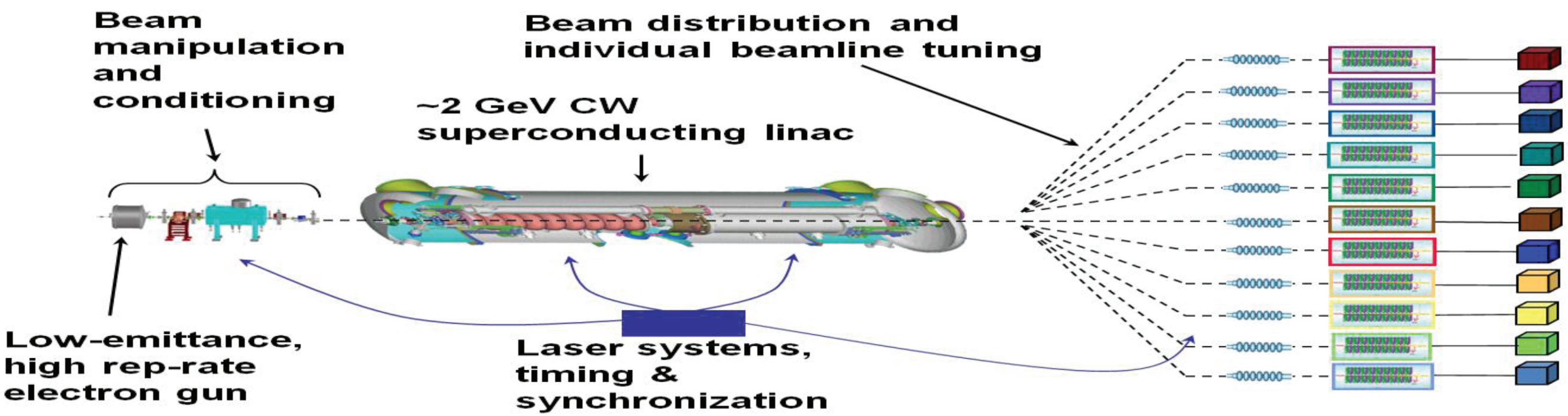

Ref: J. Corlett et al., 2013

- previous studies were done with injector and linac optimization separately
- optimizing the linac using the best-performing solution from the injector does not guarantee the best solution at the end of the accelerator.
- local optima may exist given the high dimension of search space
- global optimization method is needed to avoid local optimal solutions
- global start-to-end simulation is needed to allow all machine control parameters to vary simultaneously.

Global Optimization Using a Stochastic Evolutionary Method to Overcome Local Optimal Solution

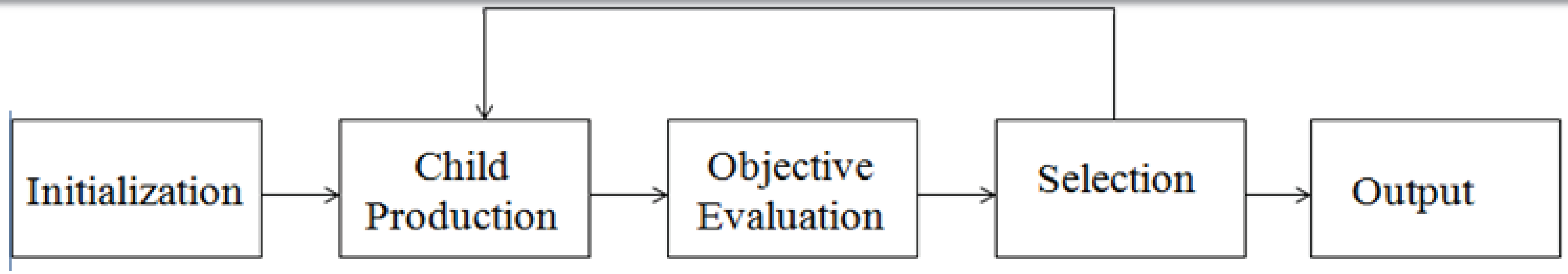

Differential Evolution Algorithm:

- Stochastic, population-based evolutionary optimization algorithm
- Easy to implement and to extend to multi-processor
- DE has been shown to be effective on a large range of classic optimization problems
  - In a comparison by Storn and Price in 1997 DE was more efficient than simulated annealing and genetic algorithms
  - Ali and Torn (2004) found that DE was both more accurate and more efficient than controlled random search
  - In 2004 Lampinen and Storn demonstrated that DE was more accurate than several other optimization methods including four genetic algorithms, simulated annealing and evolutionary programming

R. Storn and K. Price, Journal of Global Optimization 1a1:341-359, (1997).

Differential Evolution Algorithm

- A population of control parameter vectors are randomly generated from the control parameter space
- A new perturbed vector is generated for each parent by:

$$v_i = x_{i,G} + \lambda(x_{best,G} - x_{i,G}) + F(x_{r2,G} - x_{r3,G}) \longrightarrow \textit{mutation}$$

- A new trial control parameter vector is generated by:

$$U_{i,G+1} = (u_{i1,G+1}, u_{i2,G+1}, \cdots, u_{iD,G+1})$$

$$u_{ij,G+1} = \begin{cases} v_{ij}, \ if\ rand_j \le CR \ or \ j = mbr_i \\ x_{ij}, \ otherwise \end{cases} \longrightarrow \textit{cross over}$$

- If the new trial vector produces a better objective function value, it will be put into the next generation *G+1* population. Otherwise, the original parent vector is kept in the next generation population.

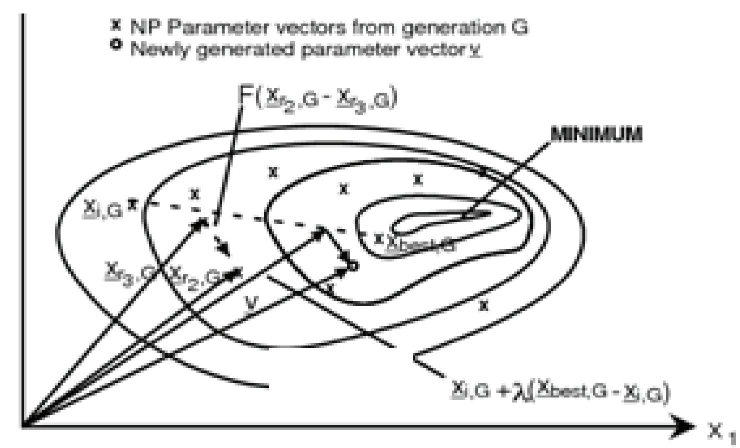

Fig.3: Two dimensional example of an objective function show generating v in scheme DE2.

v

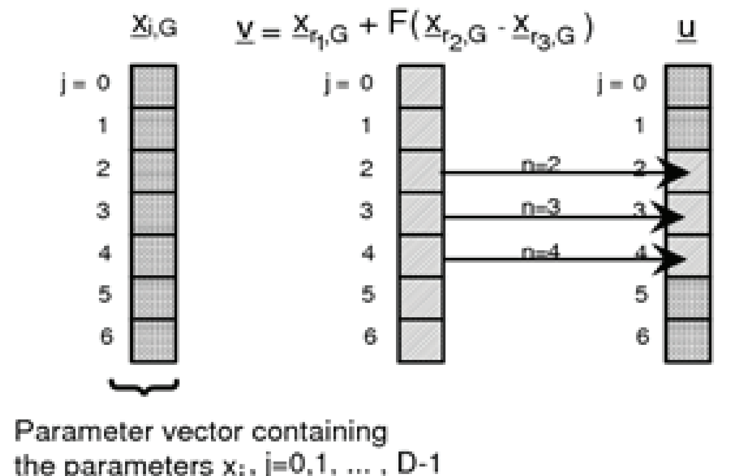

...stration of the crossover process for D=7, n=2 and L=3.

An Adaptive Unified Differential Evolution Algorithm: Reduce the Number of Mutation Strategies from 10 to 1

Some standard DE mutation strategies:

DE/rand/1: $\vec{v}_i = \vec{x}_{r1} + F_{xc}(\vec{x}_{r2} - \vec{x}_{r3})$

DE/rand/2: $\vec{v}_i = \vec{x}_{r1} + F_{xc}(\vec{x}_{r2} - \vec{x}_{r3}) + F_{xc}(\vec{x}_{r4} - \vec{x}_{r5})$

DE/current-to-best/1: $\vec{v}_i = \vec{x}_i + F_{cr}(\vec{x}_b - \vec{x}_i) + F_{xc}(\vec{x}_{r1} - \vec{x}_{r2})$

DE/current-to-rand/1: $\vec{v}_i = \vec{x}_i + F_{cr}(\vec{x}_{r1} - \vec{x}_i) + F_{xc}(\vec{x}_{r2} - \vec{x}_{r3})$

DE/rand-to-best/1: $\vec{v}_i = \vec{x}_i + F_{cr}(\vec{x}_b - \vec{x}_i) + F_{xc}(\vec{x}_{r2} - \vec{x}_{r3})$

. . .

randomly chosen solutions

current solution

best solution

Unified DE mutation strategy (uDE):

$$\vec{v}_i = \vec{x}_i + F_1(\vec{x}_b - \vec{x}_i) + F_2(\vec{x}_{r1} - \vec{x}_i) + F_3(\vec{x}_{r2} - \vec{x}_{r3}) + F_4(\vec{x}_{r4} - \vec{x}_{r5})$$

Encompasses standard DE mutation strategies as special cases. Four control parameters + CR.

$$F_{j,i}^{G+1} = \begin{cases} F_{jmin} + r_{j1}(F_{jmax} - F_{jmin}), & \text{if} \quad r_{j2} < \tau_j \\ F_{j,i}^{G}, & \text{otherwise} \end{cases}$$

J. Qiang and C. Mitchell, in OO digest, 2015.

A Pseudo Code of the Adaptive Unified Differential Evolution Algorithm

Step 1: Generate a set of initial control parameters (F_1, F_2, F_3, F_4, Cr) from random uniform sampling in the interval [0,1]. Generate a set of initial population members by randomly sampling NP points within the feasible control parameter space $\vec{x}$ and evaluate their objective function values $f(\vec{x})$. Set the generation number $G = 0$.

Step 2: While the stopping criterion is not satisfied, Do:

For i = 1 to NP (for each target parent solution $\vec{x}_i$):

Step 2.1: Mutation

Find a set of control parameters (for j=1,2,3,4):

$$F_{j,i}^{G+1} = \begin{cases} F_{jmin} + r_{j1}(F_{jmax} - F_{jmin}), & \text{if } \; r_{j2} < \tau_j \\ F_{1,i}^{G}, & \text{otherwise} \end{cases}$$

$$Cr_i^{G+1} = \begin{cases} Cr_{min} + r_3(Cr_{max} - Cr_{min}), & \text{if } \; r_4 < \tau_5 \\ Cr_i^{G}, & \text{otherwise} \end{cases}$$

Find a mutant solution vector using the uDE mutation strategy:

Step 2.2: Crossover

Generate a new trial solution $\vec{U}_i(u_{i1}, u_{i2}, \cdots, u_{iD})$ through a binominal crossover scheme:

$u_{ij} = v_{ij}$ if $\text{rand}_{ij}[0,1] \leq Cr_i^{G+1}$ *or* $j = j_{\text{rand}}$,

otherwise $u_{ij} = x_{ij}$.

Step 2.3: Selection

Evaluate the objective function of the trial solution $f(\vec{U}_i)$.

If $f(\vec{U}_i) \leq f(\vec{x}_i)$, then $\vec{x}_{i,G+1} = \vec{U}_i$,

else $\vec{x}_{i,G+1} = \vec{x}_{i,G}$.

End For

$G = G + 1$

End While

Improve the uDE Using 14 Multi-Variable Test Function Tuning

2.1.1. *F_1: Shifted Sphere Function*

$$F_1(\mathbf{x}) = \sum_{i=1}^{D} z_i^{\,2} + f\_bias_1 \,, \mathbf{z} = \mathbf{x} - \mathbf{o} \,, \mathbf{x} = [x_1, x_2, ..., x_D]$$

2.1.2. *F_2: Shifted Schwefel's Problem 1.2*

$$F_2(\mathbf{x}) = \sum_{i=1}^{D} (\sum_{j=1}^{i} z_j)^2 + f\_bias_2 \,, \ \mathbf{z} = \mathbf{x} - \mathbf{o} \,, \mathbf{x} = [x_1, x_2, ..., x_D]$$

2.1.3. *F_3: Shifted Rotated High Conditioned Elliptic Function*

$$F_3(\mathbf{x}) = \sum_{i=1}^{D} (10^6)^{\frac{i-1}{D-1}} z_i^2 + f\_bias_3 \,, \ \mathbf{z} = (\mathbf{x} - \mathbf{o}) * \mathbf{M} \,, \mathbf{x} = [x_1, x_2, ..., x_D]$$

2.1.4. *F_4: Shifted Schwefel's Problem 1.2 with Noise in Fitness*

$$F_4(\mathbf{x}) = (\sum_{i=1}^{D} (\sum_{j=1}^{i} z_j)^2) * (1 + 0.4 \left| N(0,1) \right|) + f\_bias_4 \,, \ \mathbf{z} = \mathbf{x} - \mathbf{o} \,, \mathbf{x} = [x_1, x_2, ..., x_D]$$

2.1.5. *F_5: Schwefel's Problem 2.6 with Global Optimum on Bounds*

$$f(\mathbf{x}) = \max\{\left|x_1 + 2x_2 - 7\right|, \left|2x_1 + x_2 - 5\right|\}, i = 1, ..., n \,, \ \mathbf{x}^* = [1,3] \,, f(\mathbf{x}^*) = 0$$

Extend to D dimensions:

$$F_5(\mathbf{x}) = \max\{\left|\mathbf{A}_i \mathbf{x} - \mathbf{B}_i\right|\} + f\_bias_5 \,, i = 1, ..., D \,, \mathbf{x} = [x_1, x_2, ..., x_D]$$

2.2.1. *F_6: Shifted Rosenbrock's Function*

$$F_6(\mathbf{x}) = \sum_{i=1}^{D-1} (100(z_i^2 - z_{i+1})^2 + (z_i - 1)^2) + f\_bias_6 \,, \ \mathbf{z} = \mathbf{x} - \mathbf{o} + 1 \,, \mathbf{x} = [x_1, x_2, ..., x_D]$$

2.2.2. *F_7: Shifted Rotated Griewank's Function without Bounds*

$$F_7(\mathbf{x}) = \sum_{i=1}^{D} \frac{z_i^{\,2}}{4000} - \prod_{i=1}^{D} \cos(\frac{z_i}{\sqrt{i}}) + 1 + f\_bias_7 \,, \ \mathbf{z} = (\mathbf{x} - \mathbf{o}) * \mathbf{M} \,, \ \mathbf{x} = [x_1, x_2, ..., x_D]$$

Improve the uDE Using 14 Multi-Variable Test Function Tuning

2.2.3. *F_8: Shifted Rotated Ackley's Function with Global Optimum on Bounds*

$$F_8(\mathbf{x}) = -20\exp(-0.2\sqrt{\frac{1}{D}\sum_{i=1}^{D} z_i^2}) - \exp(\frac{1}{D}\sum_{i=1}^{D}\cos(2\pi z_i)) + 20 + e + f\_bias_8, \ \mathbf{z} = (\mathbf{x}-\mathbf{o})*\mathbf{M},$$

2.2.4. *F_9: Shifted Rastrigin's Function*

$$F_9(\mathbf{x}) = \sum_{i=1}^{D}(z_i^2 - 10\cos(2\pi z_i) + 10) + f\_bias_9, \ \mathbf{z} = \mathbf{x}-\mathbf{o}, \ \mathbf{x} = [x_1, x_2, ..., x_D]$$

2.2.5. *F_{10}: Shifted Rotated Rastrigin's Function*

$$F_{10}(\mathbf{x}) = \sum_{i=1}^{D}(z_i^2 - 10\cos(2\pi z_i) + 10) + f\_bias_{10}, \ \mathbf{z} = (\mathbf{x}-\mathbf{o})*\mathbf{M}, \mathbf{x} = [x_1, x_2, ..., x_D]$$

2.2.6. *F_{11}: Shifted Rotated Weierstrass Function*

$$F_{11}(\mathbf{x}) = \sum_{i=1}^{D}(\sum_{k=0}^{k\max}[a^k\cos(2\pi b^k(z_i+0.5))]) - D\sum_{k=0}^{k\max}[a^k\cos(2\pi b^k\cdot 0.5)] + f\_bias_{11},$$

2.2.7. *F_{12}: Schwefel's Problem 2.13*

$$F_{12}(\mathbf{x}) = \sum_{i=1}^{D}(\mathbf{A}_i - \mathbf{B}_i(\mathbf{x}))^2 + f\_bias_{12}, \mathbf{x} = [x_1, x_2, ..., x_D]$$

$$\mathbf{A}_i = \sum_{j=1}^{D}(a_{ij}\sin\alpha_j + b_{ij}\cos\alpha_j), \mathbf{B}_i(x) = \sum_{j=1}^{D}(a_{ij}\sin x_j + b_{ij}\cos x_j), \text{ for } i = 1, ..., D$$

Improve the uDE Using 14 Multi-Variable Test Function Tuning

Number	Function Name	Function Properties
F_1	Shifted sphere function	unimodal, separable
F_2	Shifted Schwefel's Problem 1.2	unimodal, non-separable
F_3	Shifted rotated high conditioned elliptic function	unimodal, non-separable
F_4	Shifted Schwefel's Problem 1.2 with noise in fitness	unimodal, non-separable, with noise
F_5	Schwefel's Problem 2.6 with global optimum on bounds	unimodal, non-separable, optimum on the boundary
F_6	Shifted Rosenbrock's function	multi-modal, non-separable, narrow valley
F_7	Shifted rotated Griewank's function without bounds	multi-modal, non-separable, no bounds
F_8	Shifted rotated Ackley's function with global optimum on bounds	multi-modal, non-separable, optimum on the boundary
F_9	Shifted Rastrigin's function	multi-modal, separable, large number of local optima
F_{10}	Shifted rotated Rastrigin's function	multi-modal, non-separable, large number of local optima
F_{11}	Shifted rotated Weierstrass function	multi-modal, non-separable, continuous but not differentiable
F_{12}	Schwefel's Problem 2.13	multi-modal, non-separable, random
F_{13}	Expanded extended Griewank's plus Rosenbrock's function	multi-modal, non-separable, expanded
F_{14}	Shifted rotated expanded Scaffer's F6	multi-modal, non-separable, expanded

Performance Comparison of Different DE Strategies with 10 and 30 Dimensional Test Problem

10 dimensional problem

Function	rand/1/bin (0.9,0.9)		rand/1/bin (0.5,0.9)		best/1/bin (0.6,0.3)		jDE		AuDE3	
	Mean	Std	Mean	Std	Mean	Std	Mean	Std	Mean	Std
F_1	0.0000000E+00	0.0000000E+00	1.1600453E-05	6.7763915E-06	0.0000000E+00	0.0000000E+00	2.2737368E-15	1.1138990E-14	0.0000000E+00	0.0000000E+00
F_2	0.0000000E+00	0.0000000E+00	5.2947817E-02	3.1812454E-02	0.0000000E+00	0.0000000E+00	8.2032011E-09	5.6288682E-09	0.0000000E+00	0.0000000E+00
F_3	2.7436183E-03	1.9246452E-03	2.7960187E+04	1.0797875E+04	1.9969938E+05	8.8750793E+04	1.8085329E+03	6.9729592E+02	2.3677544E+02	5.1772101E+02
F_4	6.5907689E-08	1.1377208E-07	8.0278412E-01	3.2090327E-01	0.0000000E+00	0.0000000E+00	4.1926821E-03	2.6378655E-03	0.0000000E+00	0.0000000E+00
F_5	3.0234581E+01	7.0282410E+00	7.5117681E+02	1.4761628E+02	0.0000000E+00	0.0000000E+00	1.5947931E+01	4.2887970E+00	0.0000000E+00	0.0000000E+00
F_6	5.6672991E+00	2.0288077E+00	1.2190600E+02	4.3514187E+01	2.0705489E+00	1.3535926E+00	2.0976418E+00	1.5543555E+00	4.7838949E-01	1.2954849E+00
F_7	5.3679379E-01	7.0823728E-02	6.3233369E-01	8.4555716E-02	1.6378389E-01	5.7131860E-02	1.4336614E-01	3.1907309E-02	8.0046650E-02	4.7315555E-02
F_8	2.0338342E+01	6.7732253E-02	2.0340375E+01	8.7961754E-02	2.0350417E+01	6.5733178E-02	2.0333058E+01	6.9860187E-02	2.0348756E+01	6.9117752E-02
F_9	2.4927923E+01	3.8553340E+00	2.4869593E+01	3.2228950E+00	1.4725394E+00	1.3531443E+00	2.1613194E+00	7.9532603E-01	0.0000000E+00	0.0000000E+00
F_{10}	3.3944239E+01	4.4434536E+00	4.1290421E+01	5.8501187E+00	1.3738418E+01	3.5896022E+00	1.7154255E+01	3.1317709E+00	6.2387856E+00	2.5361897E+00
F_{11}	8.1169937E+00	8.3923093E-01	8.9664471E+00	5.7881595E-01	6.2555724E+00	6.7614688E-01	4.9552116E+00	6.9448385E-01	2.1324491E+00	1.4317264E+00
F_{12}	6.3814388E+02	2.4652132E+02	3.3414181E+03	1.0060128E+03	1.6773491E+02	4.0512937E+02	1.1206846E+02	5.3707647E+01	4.4314780E+02	6.5549769E+02
F_{13}	2.6586147E+00	3.4527250E-01	3.4535876E+00	3.2945086E-01	6.0300527E-01	1.5142810E-01	7.1776035E-01	1.1885232E-01	5.3060953E-01	9.9485625E-02
F_{14}	3.4981003E+00	1.4757772E-01	3.7472745E+00	1.3941907E-01	3.2142822E+00	2.6952966E-01	3.3314049E+00	1.6609668E-01	2.3760892E+00	3.5611190E-01

30 dimensional problem

Function	rand/1/bin (0.9,0.9)		rand/1/bin (0.5,0.9)		best/1/bin (0.6,0.3)		jDE		AuDE3	
	Mean	Std	Mean	Std	Mean	Std	Mean	Std	Mean	Std
F_1	4.0042068E-02	8.8307992E-03	1.0409654E+04	1.2104588E+03	5.4569682E-14	1.9559423E-14	5.3842086E-12	2.1210759E-12	0.0000000E+00	0.0000000E+00
F_2	1.5757241E+03	2.9986085E+02	3.3304339E+04	3.3040277E+03	2.8456738E+01	2.1763623E+01	1.2267751E+02	1.9971381E+01	7.9580786E-14	3.9382276E-14
F_3	2.4548382E+07	4.2367728E+06	2.0209261E+08	3.6717114E+07	2.8650801E+07	8.7024844E+06	4.2126081E+06	9.0229399E+05	1.4104564E+05	5.6480228E+04
F_4	8.9192323E+03	1.5487786E+03	4.0898995E+04	3.8311927E+03	4.4456661E+02	3.5711772E+02	5.9860186E+03	1.3586903E+03	9.8061342E+00	3.0106320E+01
F_5	9.4191660E+03	5.8526015E+02	1.8207668E+04	1.2946165E+03	1.6502553E+03	4.0466493E+02	5.1414490E+03	7.3617359E+02	2.2921628E+03	5.1893203E+02
F_6	1.5925815E+04	4.1294933E+03	8.7971860E+08	2.2523826E+08	2.9464409E+01	2.0417706E+01	3.5691109E+01	3.4591071E+00	1.9135795E+00	1.9917166E+00
F_7	1.0166459E+00	2.3860761E-02	5.2188218E+02	5.9920405E+01	1.2116428E-02	1.0649478E-02	6.2153108E-02	1.9692525E-02	1.5553466E-02	1.6031365E-02
F_8	2.0949387E+01	4.7929997E-02	2.0952678E+01	3.7664812E-02	2.0939889E+01	4.3785670E-02	2.0942710E+01	4.5859964E-02	2.0925805E+01	4.1211114E-02
F_9	2.2875580E+02	1.1624656E+01	2.7182950E+02	1.1788136E+01	9.7903961E+00	3.4544417E+00	4.3379156E+01	6.0438936E+00	6.0493503E+00	4.3680387E+00
F_{10}	2.5627592E+02	1.1178713E+01	3.4069565E+02	1.3533140E+01	1.6335374E+02	1.7418266E+01	1.9153300E+02	1.3487459E+01	4.9181750E+01	1.0619879E+01
F_{11}	3.9625818E+01	1.0999765E+00	3.9586892E+01	9.2565013E-01	3.7911211E+01	1.0955156E+00	2.7922660E+01	1.1772193E+00	1.5619760E+01	3.2688980E+00
F_{12}	3.9682312E+05	4.4826984E+04	6.9160653E+05	7.3840596E+04	7.8503639E+03	1.0178754E+04	3.7835219E+04	5.6300539E+03	2.4872612E+03	3.3555087E+03
F_{13}	2.1428267E+01	1.1650938E+00	3.9428286E+01	3.6998405E+00	7.7156768E+00	7.5339803E-01	6.0425845E+00	5.8237527E-01	3.7508460E+00	3.6730826E-01
F_{14}	1.3357126E+01	1.5099584E-01	1.3469751E+01	1.0284091E-01	1.3251791E+01	1.3541026E-01	1.2910809E+01	1.5619979E-01	1.2519872E+01	3.3397551E-01

Performance Comparison of Different DE Strategies with 50 Dimensional Test Problem

Function	rand/1/bin (0.9,0.9)		rand/1/bin (0.5,0.9)		best/1/bin (0.6,0.3)		jDE		AuDE3	
	Mean	Std	Mean	Std	Mean	Std	Mean	Std	Mean	Std
F_1	3.0927386E+03	3.3806897E+02	5.8565996E+04	3.3438702E+03	7.0485839E-14	2.4276865E-14	9.7900730E-04	1.9327500E-04	0.0000000E+00	0.0000000E+00
F_2	5.3784094E+04	5.5778455E+03	1.1253028E+05	8.7430565E+03	1.6005087E+04	3.0178019E+03	1.3310258E+04	1.5506144E+03	1.7958065E-04	2.5805315E-04
F_3	3.4245986E+08	5.7162253E+07	1.0891557E+09	1.3447534E+08	1.0730390E+08	1.9084991E+07	4.0242215E+07	8.4701652E+06	5.0050682E+05	1.9314595E+05
F_4	7.3229680E+04	5.7847085E+03	1.2960611E+05	7.6975439E+03	2.8131986E+04	5.1831596E+03	4.6937176E+04	4.3890970E+03	1.0955475E+03	8.7681772E+02
F_5	2.2193246E+04	1.4385840E+03	3.1059695E+04	1.4857210E+03	4.0664744E+03	7.8421179E+02	1.4083438E+04	1.0919037E+03	5.2945908E+03	9.3906237E+02
F_6	2.1235168E+08	4.0623867E+07	1.6371570E+10	2.5799614E+09	5.9170498E+01	2.5931487E+01	4.1049263E+02	5.5862000E+01	2.8137956E+00	2.0888036E+00
F_7	2.9435586E+02	2.3509047E+01	2.4503718E+03	1.7207500E+02	3.5477374E-03	5.3555807E-03	6.4442528E-01	4.5368334E-02	5.6083296E-03	9.6948211E-03
F_8	2.1142240E+01	3.0595834E-02	2.1136908E+01	3.1511796E-02	2.1136844E+01	3.2365326E-02	2.1144190E+01	4.4635915E-02	2.1122542E+01	3.2206483E-02
F_9	4.9859346E+02	1.6299490E+01	6.0849638E+02	1.5217194E+01	3.8286541E+01	3.7246640E+01	1.5887065E+02	1.3732574E+01	4.2226030E+01	1.7862920E+01
F_{10}	6.0219018E+02	1.9609180E+01	8.3051164E+02	3.0416330E+01	3.6701324E+02	1.7874542E+01	4.9269444E+02	4.3478100E+01	1.1441995E+02	2.2162231E+01
F_{11}	7.3080034E+01	1.0969651E+00	7.2906533E+01	1.6662393E+00	7.1787659E+01	1.4045202E+00	5.7315084E+01	1.7626651E+00	3.9944311E+01	1.0455411E+01
F_{12}	2.3216155E+06	1.7478052E+05	3.7863579E+06	3.0129766E+05	1.7232857E+04	1.1055801E+04	2.6931807E+05	3.1723774E+04	9.4551459E+03	7.9832132E+03
F_{13}	5.6457019E+01	3.2638241E+00	2.1127535E+02	2.8863691E+01	2.1405098E+01	1.0925048E+00	1.6828538E+01	1.1329713E+00	1.0119648E+01	7.5038179E-01
F_{14}	2.3082455E+01	1.6783775E-01	2.3233219E+01	1.3943413E-01	2.2943825E+01	1.3336836E-01	2.2683903E+01	1.4716163E-01	2.2254733E+01	3.8187439E-01

Retune uDE with 3 control variables shows better performance than several standard DEs and the jDE!

Evolution of the Average Error in the Objective Value for the First Four Test Functions

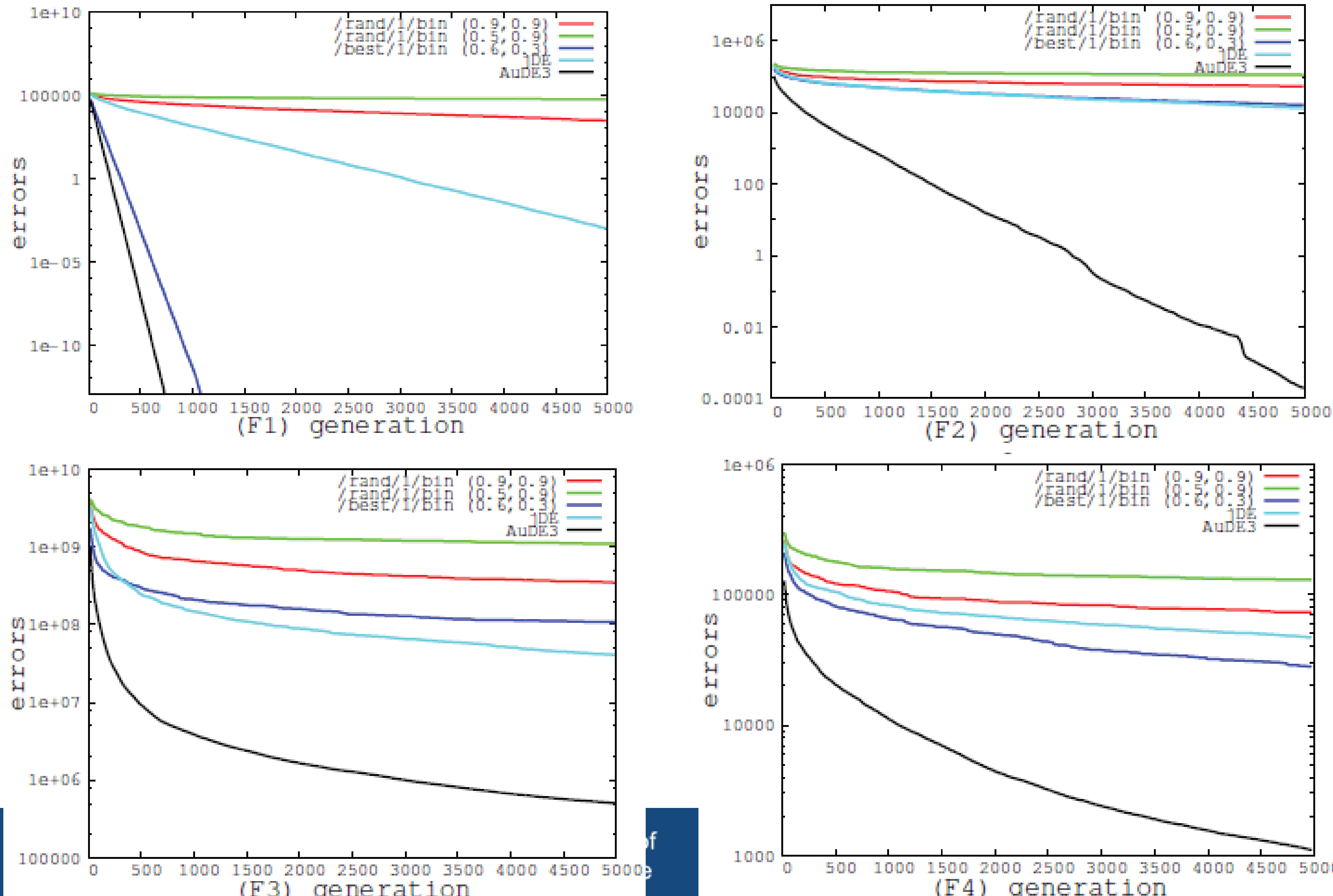

Accelerator Design Needs Multi-Objective Optimization

$$\min_{x} \begin{cases} f_1(x) \\ \dots \\ f_n(x) \end{cases} \quad \textit{subject to} \;\; g_i(x) \le 0,\, h_i(x) = 0,$$

Examples:

- cost, performance
- injector: emittance, peak current
- linac: peak current, energy spread

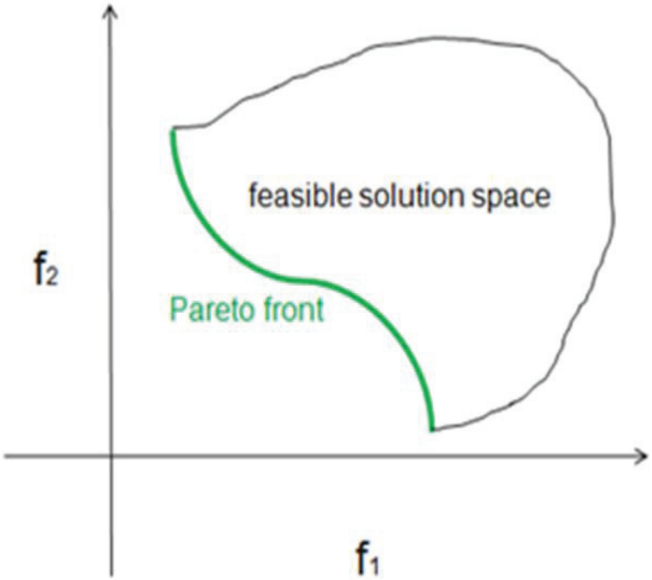

❖The goal of multi-objective optimization is to find the **Pareto front** in the objective function solution space.
❖The **Pareto front** is a set of non-dominated solutions within the whole feasible solution space.
❖A non-dominated solution is a solution that at least one of its objective function value is less than the same objective function in other solutions.

A Variable Population External Storage Multi-Objective Differential Evolution Algorithm (VPES-MODE)

- Step 1: Define the minimum parent size (Npmin), the maximum size (Npmax), and the maximum size of the external storage (Npext).
- Step 2: Generate initial Npini population of control parameter vectors randomly from the entire solution space.
- Step 3: Produce offspring population using the unified differential evolutionary algorithm.
- Step 3: Check the new population against boundary conditions and constraints.
- Step 4: Combine the new population with the existing parent population from external storage. Nondominated solutions (Ndom) are found from this group of solutions and min(Ndom, Npext) of solutions are put back into external storage. Pruning is used if Ndom > Npext. Np parent solutions are selected from this group of solutions for next generation production.
  If Npmin ≤ Ndom ≤ Npmax, Np = Ndom;
  If Ndom < Npmin, Np = Npmin;
  If Ndom > Npmax, Np = Npmax.
- Step 5: If the stopping condition is met, stop. Otherwise, return to Step 2.

Test with an Analytical Solution

$$f_1(\mathbf{x}) = x_1 \qquad x_1 \in [0,1]$$
$$f_2(\mathbf{x}) = g(\mathbf{x})\left[1 - (x_1/g(\mathbf{x}))^2\right] \qquad x_i = 0,$$
$$g(\mathbf{x}) = 1 + 9\left(\sum_{i=2}^{n} x_i\right)/(n-1) \qquad i = 2,\ldots,n$$

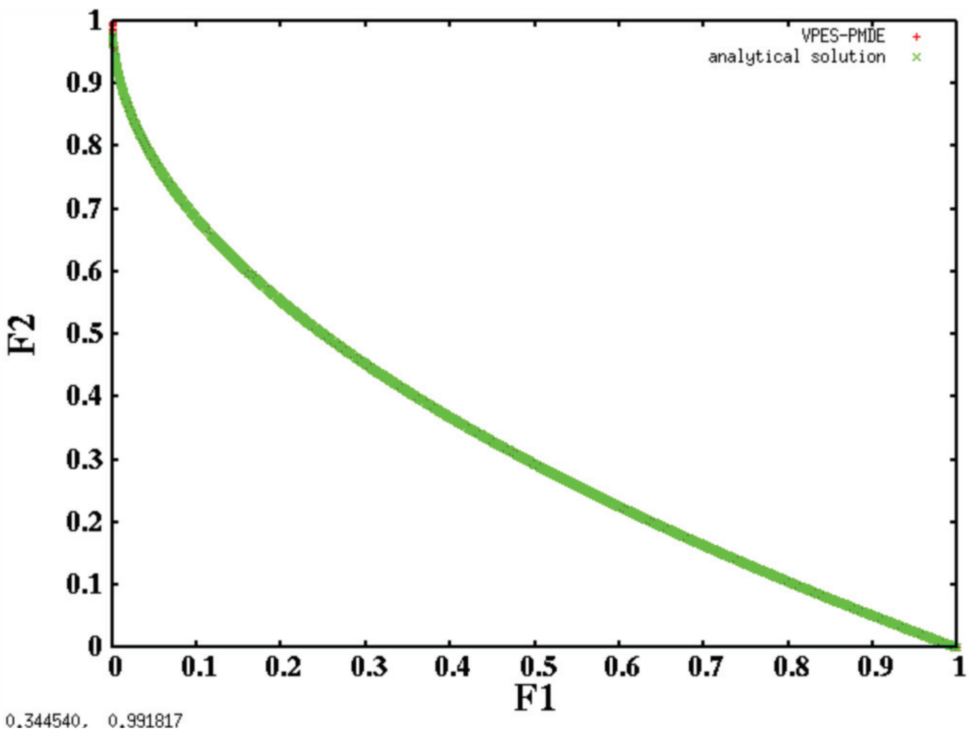

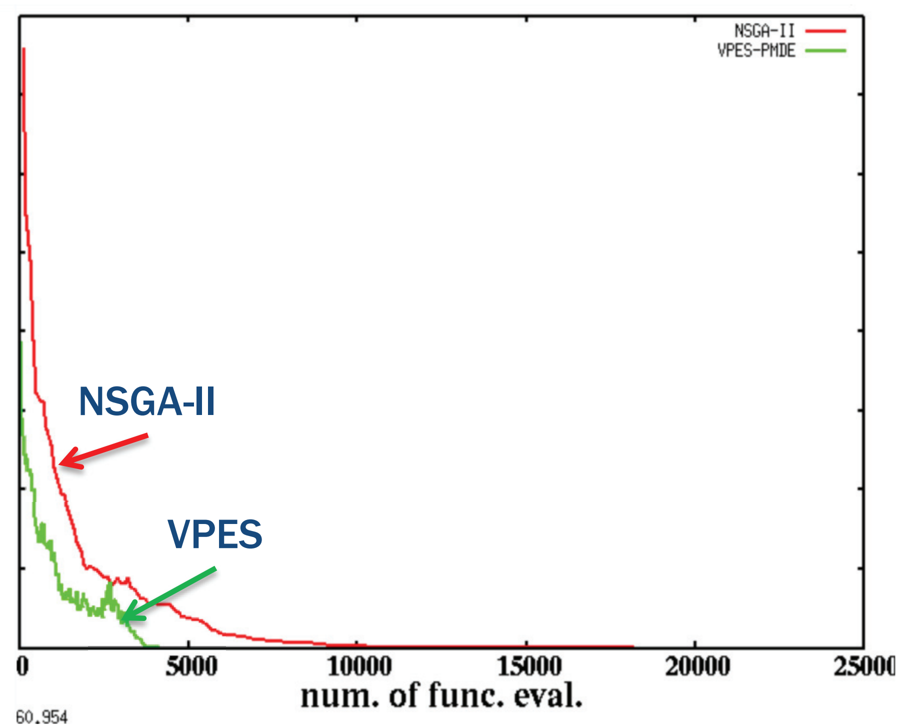

Start-to-End Beam Dynamics Simulation Using the Parallel Multi-Physics Code Suite: IMPACT

- Some major features:
  - Z dependent and T dependent tracking
  - Detailed 3D RF accelerating and focusing model, dipole, solenoid, multipole, …
  - Multiple charge states, multiple bunches
  - Multiple space-charge solvers: 3D shifted-integrated Green's function, 3D spectral finite difference multigrid space-solver, …
  - Structure + resistive wall wakefields
  - CSR/ISR
  - Gas ionization
  - Photo-electron emssion
  - Machine errors and steering
- Can be used to model beam dynamics in:
  - Photoinjectors
  - Ion beam formation and extraction
  - RF linacs
  - Rings

An Example of Start-to-End Beam Dynamics Simulation of the LCLS Microbunching Experiments

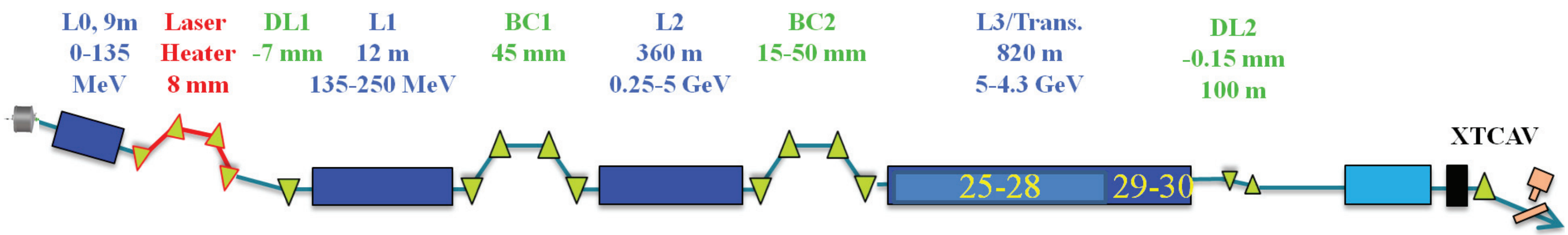

- Integrated injector and linac simulation using a single code
- Fully 3D time-dependent simulation in the injector
- Fully 3D position dependent simulation in the linac
- The multi-physics model includes:
  - 5^{th} order single particle tracking
  - self-consistent 3D space-charge effects,
  - 1D CSR effects, ISR effects
  - structure and resistive wall wakefields

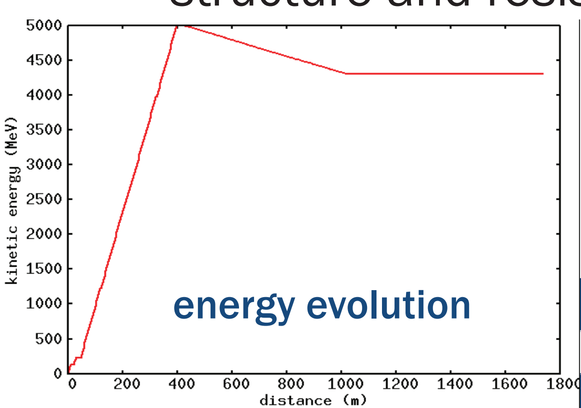

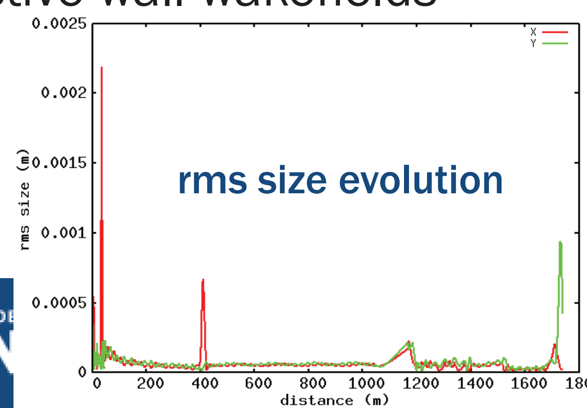

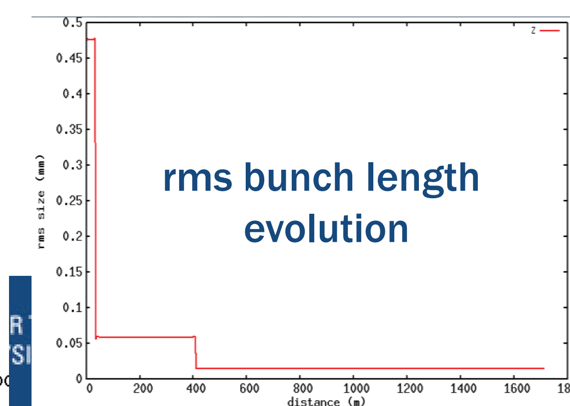

Final Longitudinal Phase Space Distribution

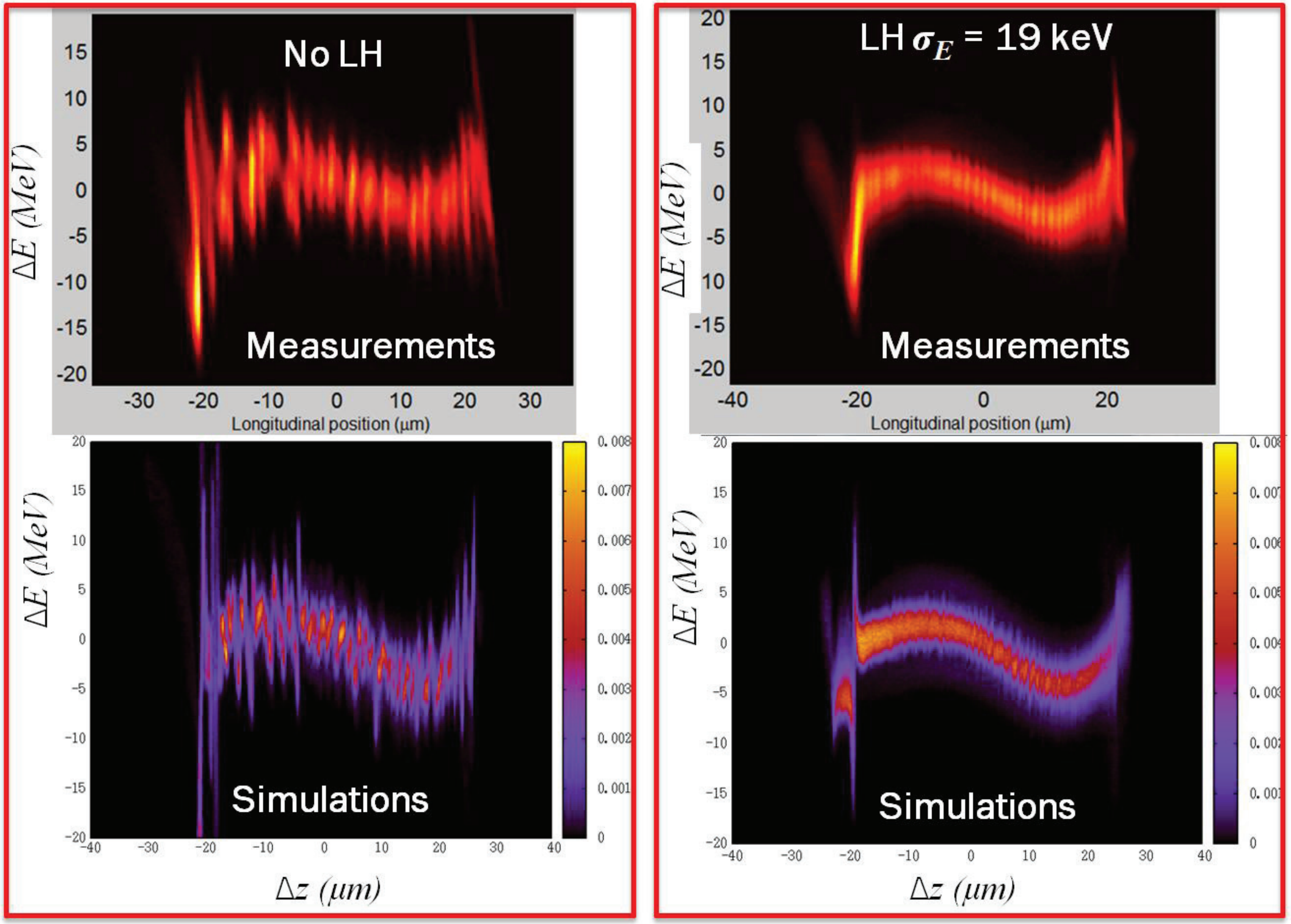

In collab.
Y. Ding et al.
at SLAC,
WEPOB30

Couple/Decouple Transverse and Longitudinal Beam Dynamics in Global Start-to-End Optimization

Ideal beam: small emittance, small energy spread, high peak current

Injector <= ~100 MeV: longitudinal and transverse motion tightly coupled

optimize simultaneously transverse and longitudinal beam dynamics

injector

Linac >= ~100 MeV: longitudinal motion is nearly frozen except in BCs

Opt. transverse beam dynamics

Opt. longitudinal beam dynamics

linac

A Diagram of Parallel Start-to-End Beam Dynamics Optimization

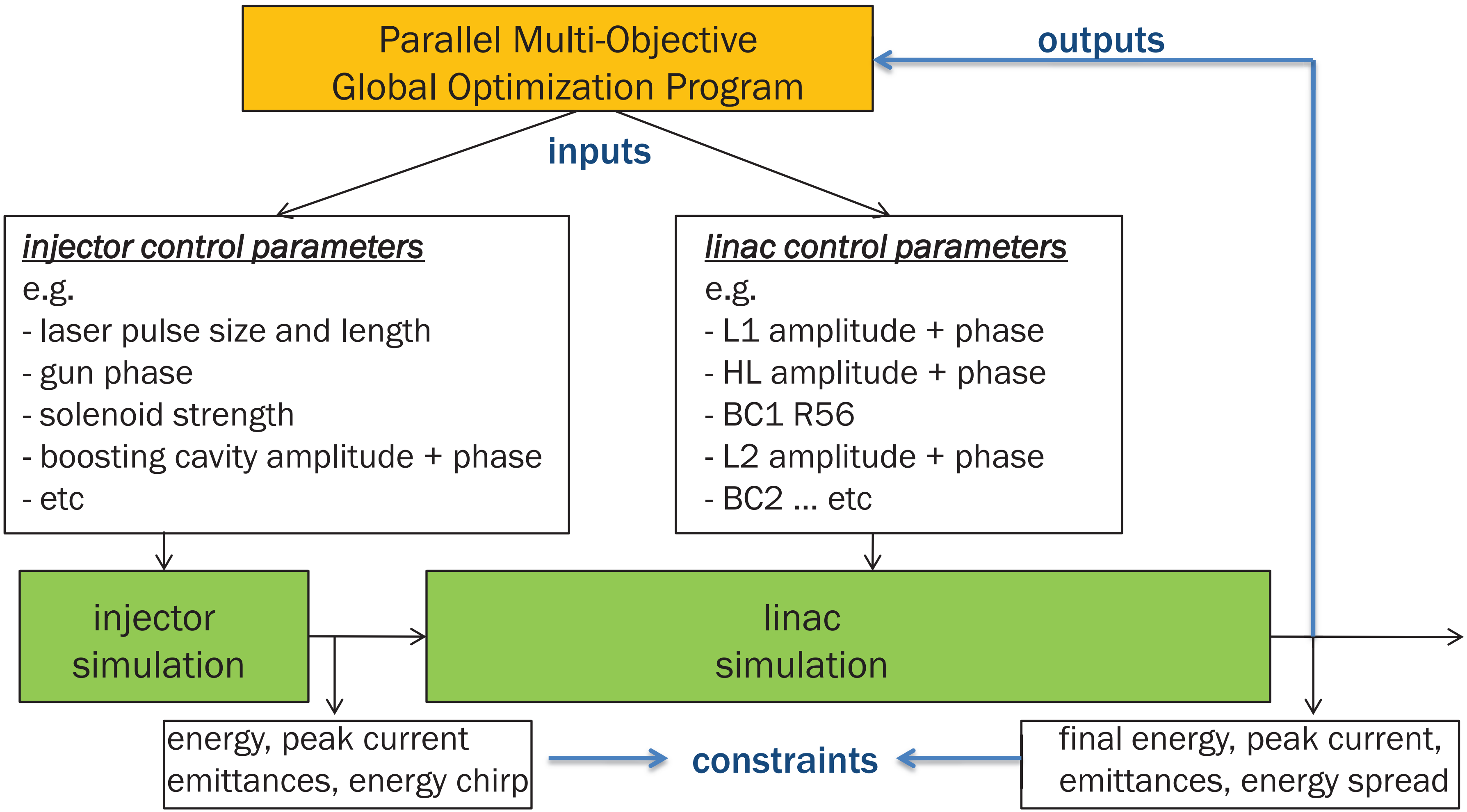

Application to an LCLS-II Design Study

A Layout of the LCLS-II Accelerator

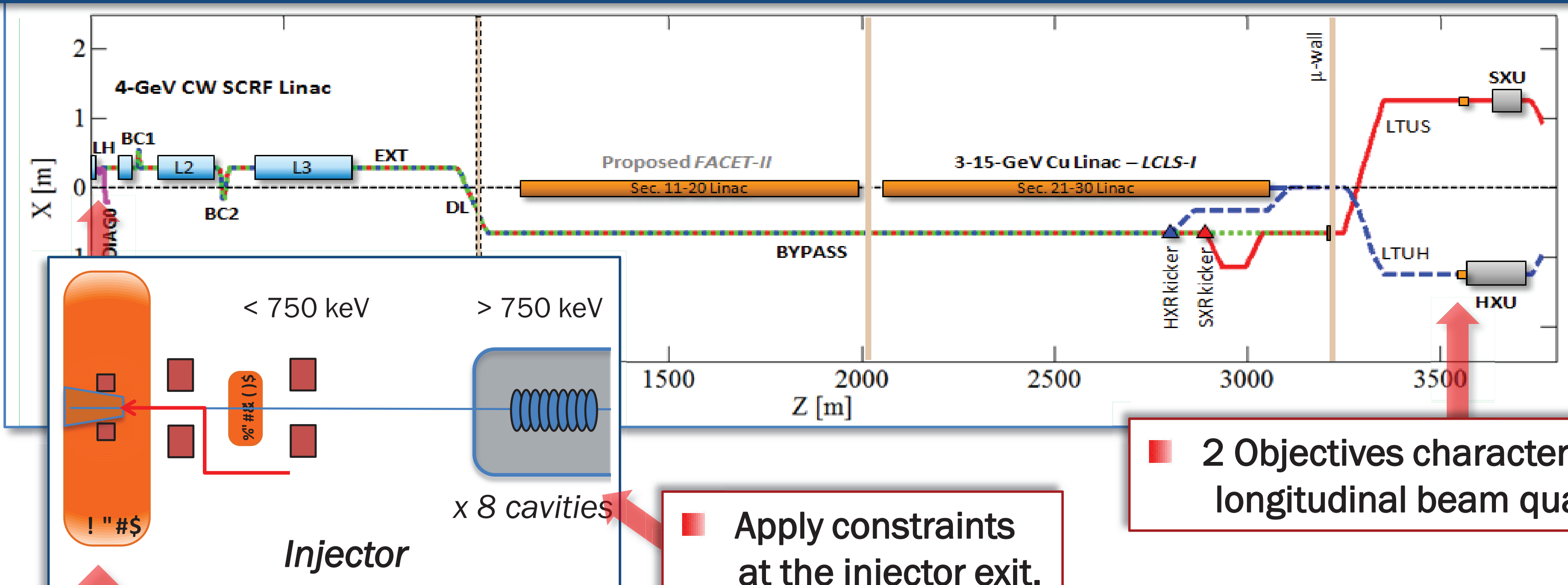

- Apply constraints at the injector exit.
- 2 Objectives characterize longitudinal beam quality.
- Allow beam properties at the cathode to vary.

- 1 MHz repetition rate to generate coherent x-ray radiation between 200 eV to 5 keV
- Injector consists of a VHF normal conducting gun, buncher, and boosting cavities
- Linac consists fo 3 superconducting cavity sections, a 3rd harmonic linearizer section, a laser heater and two bunch compressors.

Multi-Objective Global Optimization with 20 pC Charge

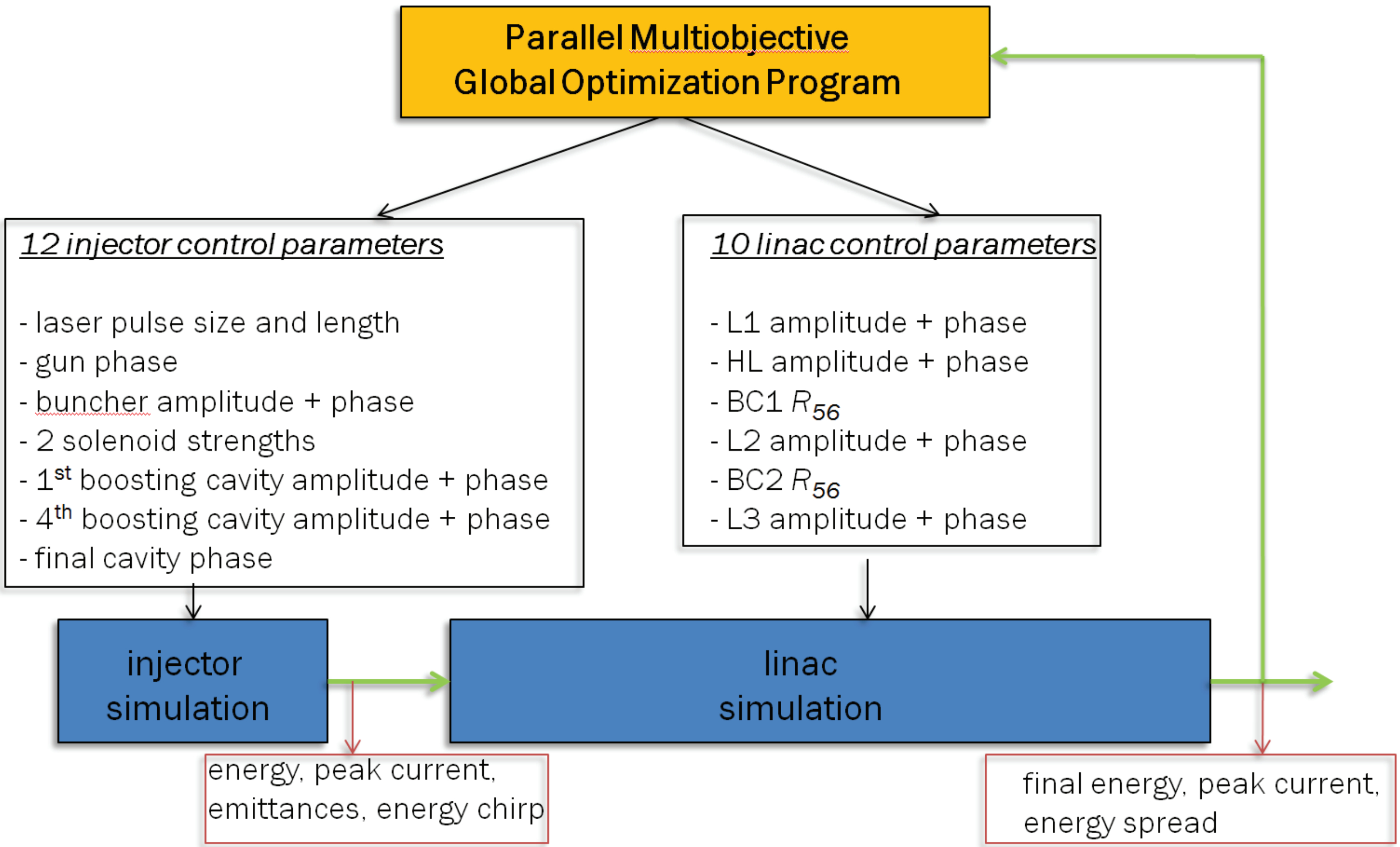

Multi-Objective Injector Beam Dynamics Optimization with 20 pC Charge

Two optimization objectives at the injector exit:

- rms bunch length
- transverse rms emittance

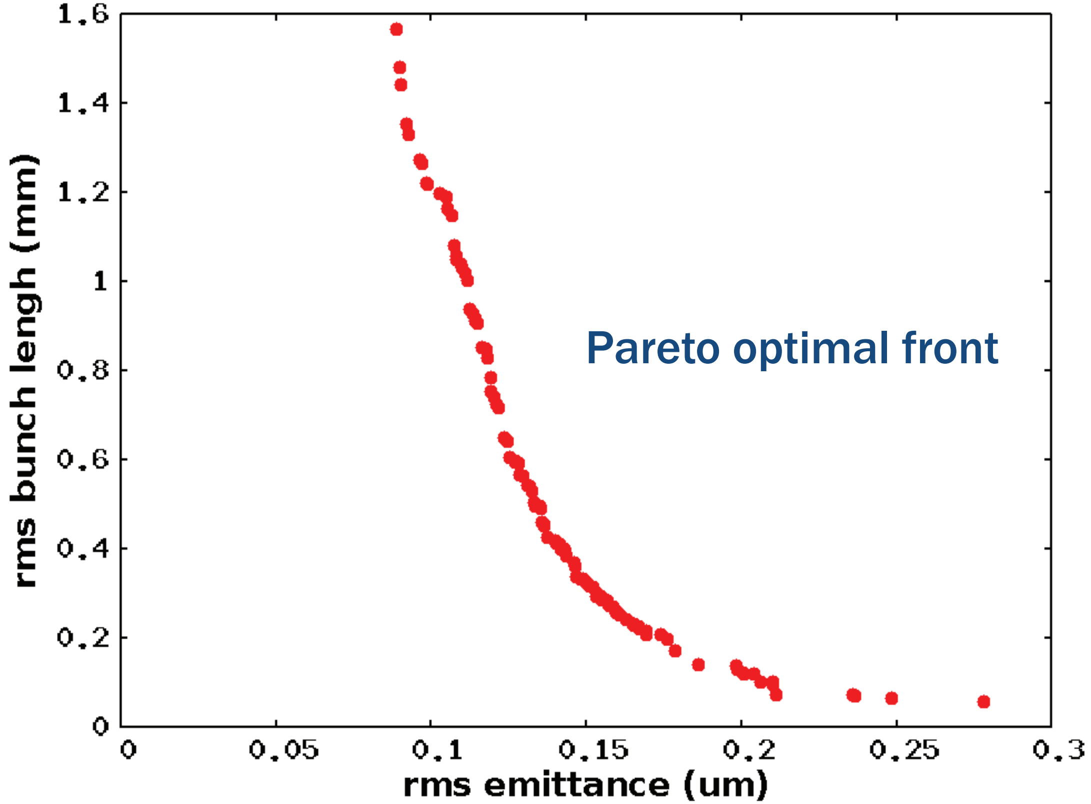

Multi-Objective Start-to-End Beam Dynamics Optimization with 20 pC Charge

- Two optimization objectives at the entrance of undulator:
  - fraction of the charge inside a window [-7,9] um
  - rms energy spread inside the window
- Combine the 12 dimension injector solutions with the 10 dimension linac random solutions at the 1st generation solution
- Turn outputs at the injector exit into constraints for global optimization

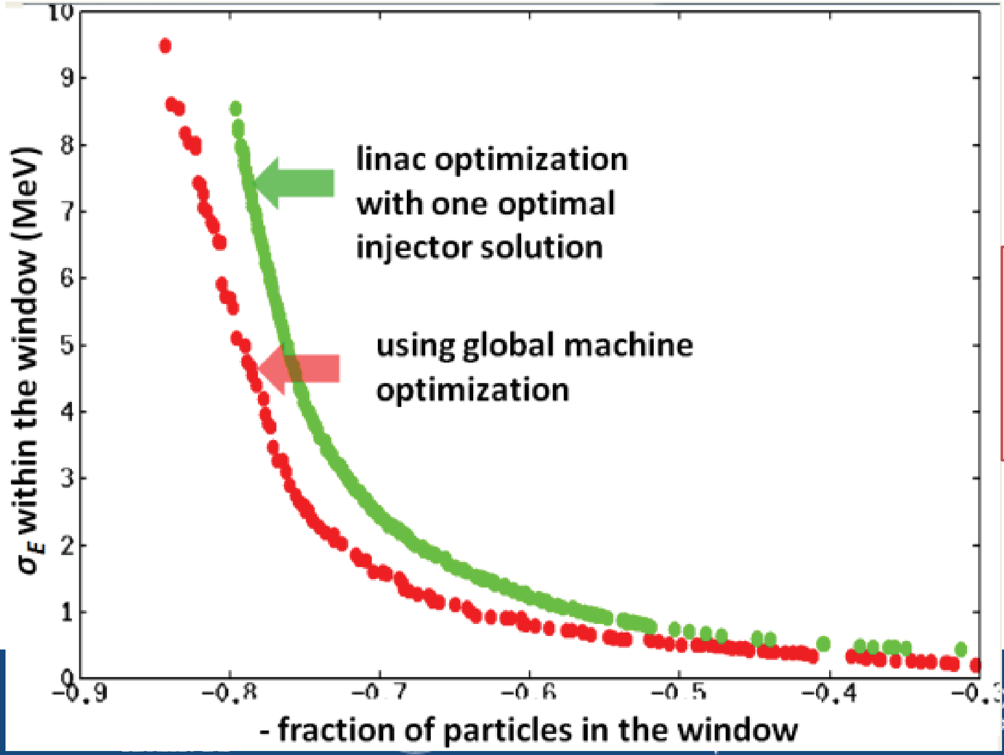

> *Global start-to-end optimization shows significant improvement of final optimal solutions.*

Improvement of Final Electron Beam Quality with Global Optimization

before optimization

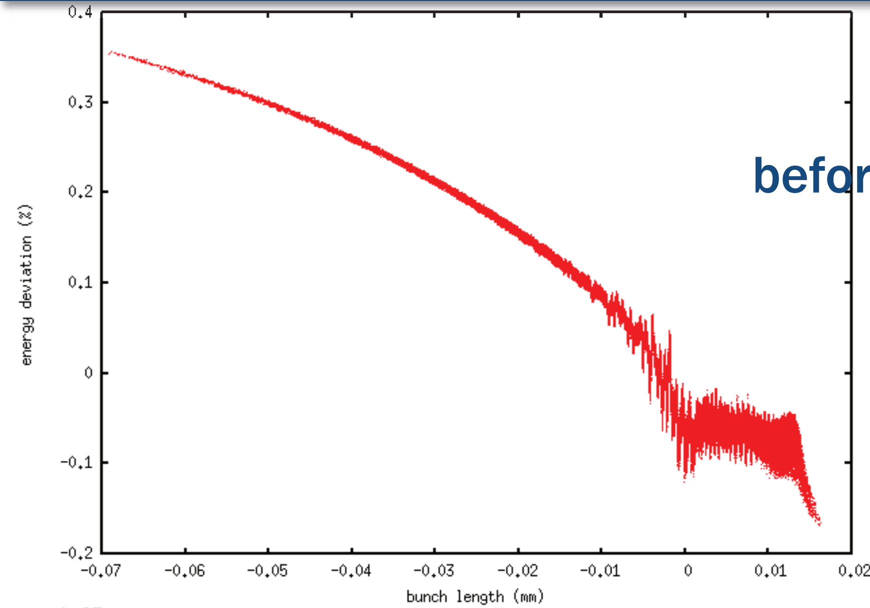

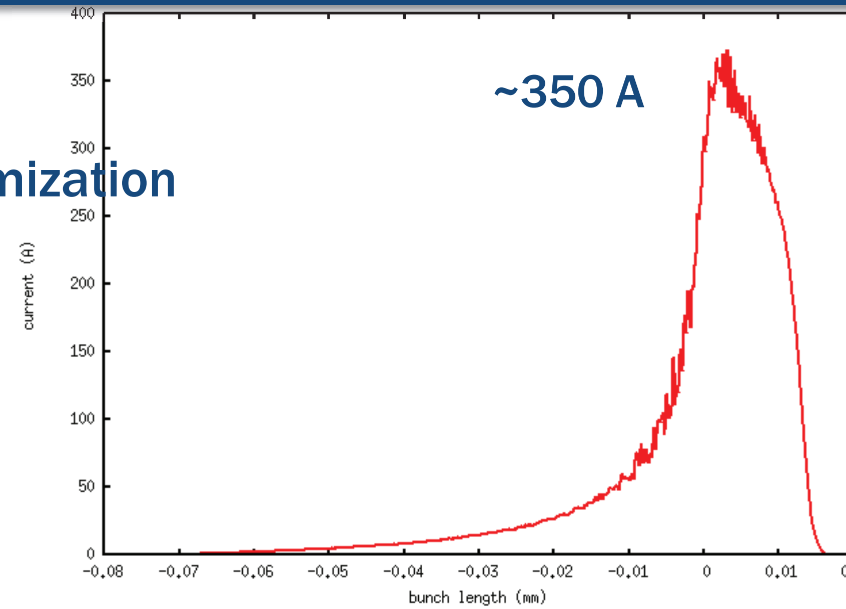

after optimization

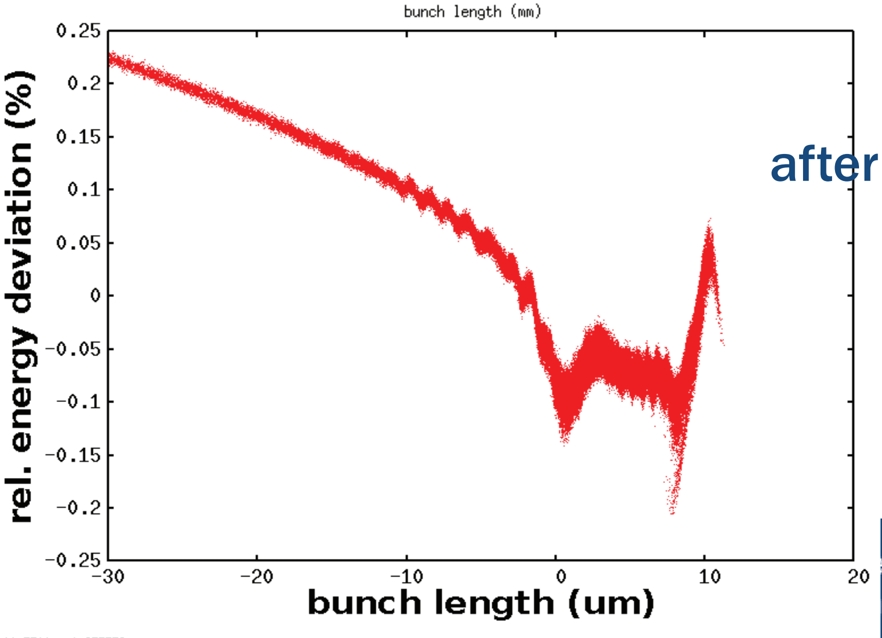

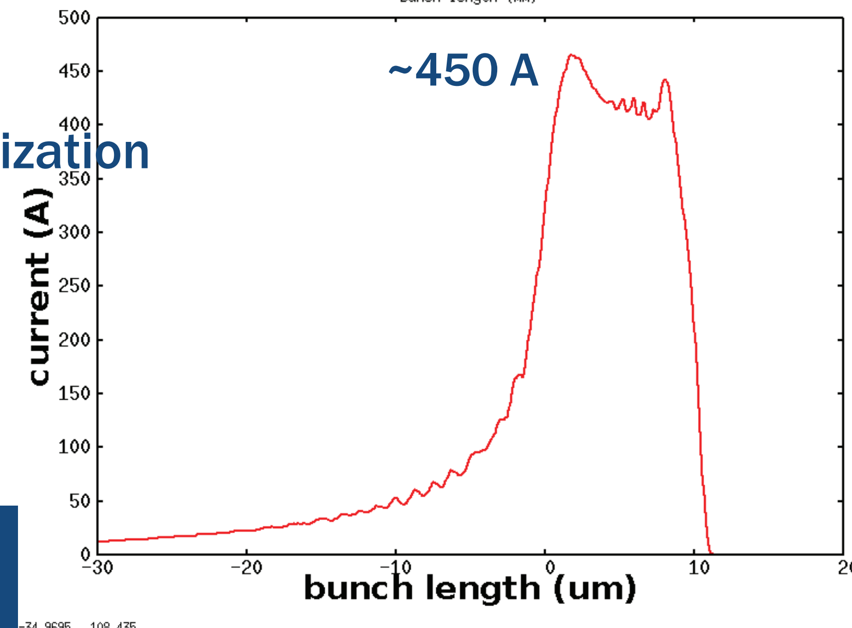

Transverse Beam Dynamics Optimization Significantly Lowers the Transverse Emittance Growth

- rematching the lattice including 3D space-charge effects
  - 1^{st} 5 quads at the exit of the injector
  - 4 quads before LH
  - 4 quads after LH
  - 4 quads after BC1

before optimization

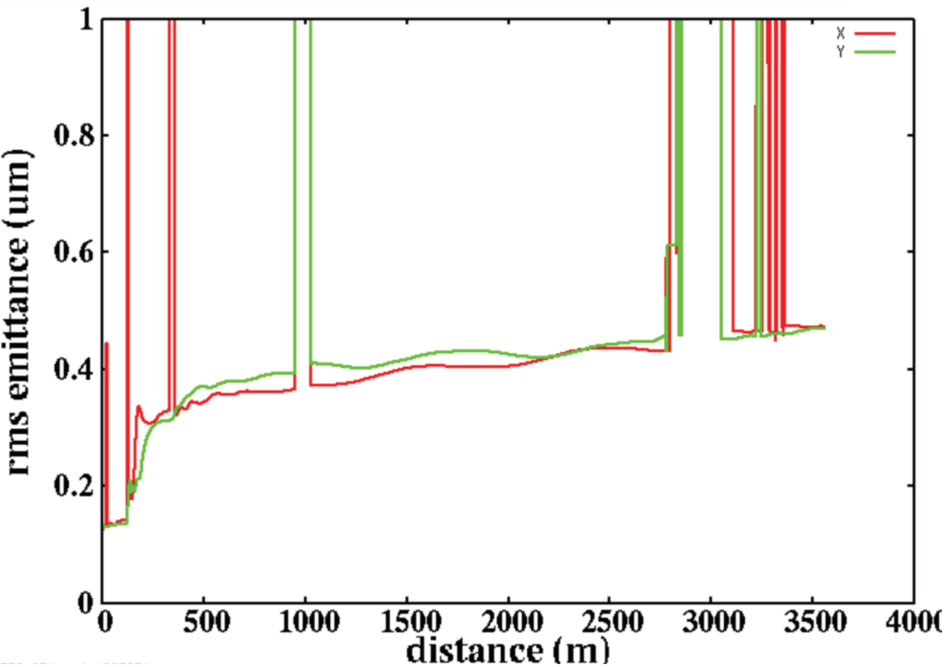

after optimization

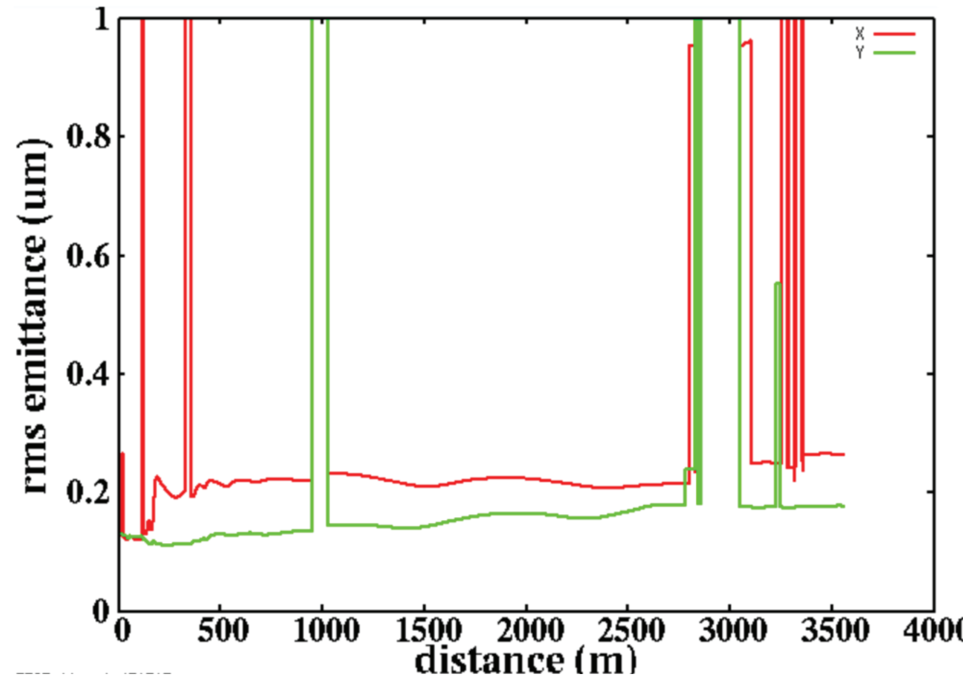

Conclusions

- Next generation x-ray FEL accelerator design needs global optimization to attain final optimal solution.
- Multi-objective start-to-end beam dynamics optimization is doable with advanced optimization algorithm and beam dynamics simulation tool.
- One application example shows significantly improvement of final electron beam quality, which might lead to “more than 80% improvement of the final 5 keV radiation energy.”

Acknowledgements

We would like to thank the LCLS-II accelerator physics design team for the 20pC global optimization application study. This work is supported by the Director of the Office of Science of the US Department of Energy under Contract no. DEAC02-05CH11231. We have used computer resources at the National Energy Research and Scientific Computing (NERSC) center.

Thank You!